Energetics of CO2 and H2O Adsorption on Zinc Oxide

ARTICLE *in* LANGMUIR · JULY 2014

Impact Factor: 4.46 · DOI: 10.1021/la500743u · Source: PubMed

3 AUTHORS, INCLUDING:

Douglas Gouvea
University of São Paulo
112 PUBLICATIONS **856** CITATIONS
SEE PROFILE

Sergey V Ushakov
University of California, Davis
69 PUBLICATIONS **1,063** CITATIONS
SEE PROFILE

Langmuir

Article

pubs.acs.org/Langmuir

Energetics of CO_2 and H_2O Adsorption on Zinc Oxide

Douglas Gouvêa,*[,†] Sergey V. Ushakov,[‡] and Alexandra Navrotsky[‡]

[†]Department of Metallurgical and Materials Engineering, Escola Politécnica, Universidade de São Paulo, Av. Prof. Melo Moraes, 2463, São Paulo, São Paulo 05508-930, Brazil

[‡]Peter A. Rock Thermochemistry Laboratory and NEAT ORU, University of California—Davis, One Shields Avenue, Davis, California 95616, United States

Supporting Information

ABSTRACT: Adsorption of H_2O and CO_2 on zinc oxide surfaces was studied by gas adsorption calorimetry on nanocrystalline samples prepared by laser evaporation in oxygen to minimize surface impurities and degassed at 450 °C. Differential enthalpies of H_2O and CO_2 chemisorption are in the range −150 ±10 kJ/mol and −110 ±10 kJ/mol up to a coverage of 2 molecules per nm^2. Integral enthalpy of chemisorption for H_2O is −96.8 ±2.5 kJ/mol at 5.6 H_2O/nm^2 when enthalpy of water condensation is reached, and for CO_2 is −96.6 ±2.5 kJ/mol at 2.6 CO_2/nm^2 when adsorption ceases. These values are consistent with those reported for ZnO prepared by other methods after similar degas conditions. The similar energetics suggests possible competition of CO_2 and H_2O for binding to ZnO surfaces. Exposure of bulk and nanocrystalline ZnO with preadsorbed CO_2 to water vapor results in partial displacement of CO_2 by H_2O. In contrast, temperature-programmed desorption (TPD) indicates that a small fraction of CO_2 is retained on ZnO surfaces up to 800 °C, under conditions where all H_2O is desorbed, with adsorption energies near −200 kJ/mol. Although molecular mechanisms of adsorption were not studied, the thermodynamic data are consistent with dissociative adsorption of H_2O at low coverage and with several different modes of CO_2 binding.

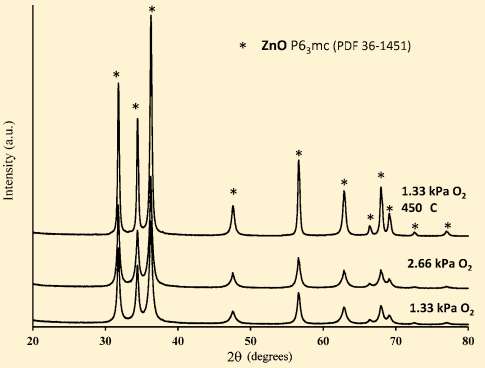

1. INTRODUCTION

Photocatalytic reduction of carbon dioxide in aqueous suspension of ZnO and other semiconductor powders was reported 35 years ago by Inoue at al.[1] In 1992, Watanabe[2] reported photosynthesis of methanol and methane from CO_2 and H_2O as alternatives to the Fischer−Tropsch synthesis and reported that ZnO is a more efficient photocatalyst than $SrTiO_3$, TiO_2, and WO_3 for that application. Recent efforts to abate atmospheric CO_2 levels and to reduce oil dependence has brought much attention to the subject of CO_2 adsorption and reaction on various substrates. This application, as well as multiple other uses of ZnO, triggered large number of theoretical and experimental research on water and CO_2 on zinc oxide surfaces.[3−7] Gas adsorption calorimetry is a well-established but not widespread method to characterize energetics of gas adsorption on surfaces of polycrystalline powders. Such calorimetric studies can also benchmark results of theoretical calculations. CO_2 adsorption calorimetry experiments on ZnO were previously performed by Aurox and Gervasini[8,9] in France. H_2O adsorption calorimetry experiments on ZnO were performed earlier at UC Davis as part of calorimetric measurements of ZnO surface energy.[10,11] In the present research, we aimed to study energetics of CO_2 and H_2O adsorption on the same well characterized samples and to evaluate effects of preadsorbed CO_2 on H_2O adsorption and vice versa. Laser evaporation was our method of choice for ZnO powder synthesis in order to alleviate surface impurities. ZnO powders were annealed at 450 °C for adsorption calorimetry for comparison with previous studies.[2,8−11] Temperature-programmed desorption (TPD) was performed to 900 °C. Mass spectrometry analysis of gas composition and adsorption calorimetry were the primary methods used to provide the basis for comparison with theoretical calculations and to resolve discrepancies in previous experimental results. With emphasis on bulk thermodynamics, we do not discuss a microscopic view of H_2O and CO_2 speciation on the ZnO surface.

2. EXPERIMENTAL SECTION

2.1. ZnO Synthesis by Laser Evaporation. ZnO nanopowders were prepared by laser evaporation using a 100 W CO_2 laser source and an atmosphere controlled chamber. Targets were fabricated by sintering 1.0 g pellets of high purity ZnO commercial powder (Alfa-Aesar 99.99%) at 1000 °C for 10 h. The final density was as high as 98%. Before evaporation samples were kept under vacuum (26.7 Pa) for 1 h and the targets were spun and heated by the laser (10 W) to eliminate any adsorbed species. High purity oxygen was used in the evaporation chamber to prevent ZnO reduction to metallic zinc during evaporation at two different pressures: 1.33 or 2.66 kPa. The highest evaporation rate was observed at 34 W at 1.33 kPa, with 300 mg ZnO nanopowder produced after 1 h of evaporation. The particles were

Received: February 24, 2014
Revised: June 25, 2014
Published: July 21, 2014

   dx.doi.org/10.1021/la500743u | Langmuir 2014, 30, 9091−9097

collected on a stainless steel substrate positioned at a distance of 70 mm from the target. The evaporation chamber was opened inside a nitrogen filled glovebox with low water content (dew point −79 °C). The powders were kept in the glovebox for further analysis. As-prepared powders were analyzed by thermogravimetry and by temperature-programmed desorption (TPD) in separate experiments. H_2O and CO_2 adsorption calorimetry, surface area, and particle size analyses were performed both for as-prepared samples and after heating to 450 °C. Calorimetric study of effects of coadsorption of H_2O and CO_2 was performed on samples prepared by laser evaporation and annealed at 450 °C. Mass spectrometry experiments on coadsorption were performed on bulk ZnO (Alfa-Aesar 99.99%) degassed at 450 °C.

2.2. Characterization. TEM images were acquired in a Philips CM-12 transmission electron microscope (TEM) operating at 100 keV. The nanopowder was sonicated in ethanol for 1 h, and the dispersion dropped on an amorphous carbon grid. Particle size was measured by TEM and the distributions were obtained by measuring the diameter at least 100 particles using ImageJ software. XRD patterns were acquired using a Bruker AXS D8 Advance instrument with CuKa radiation, K_α = 1.5418 Å to determine the crystalline phases and to measure the crystallite sizes. The specific surface area (SA) was measured by the 5 point Brunauer−Emmett−Teller (BET) method[12] with a Micromeritics ASAP 2020 gas sorption analyzer using N_2 as an adsorbent. Temperature-programmed desorption with mass spectrometric detection of evolved gases (TPD-MS) was performed on powders from laser evaporation and on bulk Alfa Aesar powder. Further experimental details are given in the Supporting Information (SI).

2.3. Gas Adsorption Calorimetry and Mass Spectrometry. Gas adsorption calorimetry and adsorption isotherm measurements were performed simultaneously at 25 °C using enough powder (about 250 mg for as-prepared powder and 130 mg for powder calcined at 450 °C) to obtain about 3 m^2 of surface inside the cell, and gas dosing was programmed to 1 μmol/m^2 doses. Calorimetric data during gas adsorption were obtained with a Setaram Sensys Calvet micro-calorimeter. The experimental procedure was described in detail previously.[13] CO_2 and H_2O adsorption calorimetry experiments were performed on as-prepared powders and after degas at 450 °C. Degas of the samples was performed using the Setaram Sensys for heating; after evacuation sample tubes were filled with oxygen at 450 °C to ensure oxidized[14−16]surfaces; thus the sample was not exposed to air before gas adsorption calorimetry.

To evaluate effects of preadsorbed H_2O on CO_2 adsorption, water adsorption measurements were first carried out on a sample degassed at 450 °C, then the sample was evacuated for ∼6 h at 25 °C and CO_2 adsorption experiments were performed. To evaluate the effect of H_2O adsorption on a surface partially covered with CO_2, a similar procedure was followed but CO_2 adsorption was performed first on the degassed surface.

In these experiments, the amount of adsorbed gas is reported by the Micromeritics ASAP 2020 software from the observed pressure decrease in incremental dosing mode. Heat effects are measured independently for each dose by the calorimeter. They are divided by the amount of adsorbed gas in that dose to yield the differential enthalpy of adsorption in kJ/mol. Coverage reached with each dose is calculated using total surface area measured by BET for the sample used for adsorption calorimetry.

For the above experiments, possible desorption of preadsorbed species must be considered. If this occurs, then adsorbed amounts will be underestimated, and differential adsorption enthalpy will be overestimated. A separate set of experiments was performed to find out if exposure to water vapor caused desorption of CO_2 from the surface of ZnO and vice versa. The heated capillary input of a MKS Cirrus 2 quadrupole mass spectrometer was connected to the manifold of the Micromeritics ASAP 2020 instrument in the port normally used to measure saturation pressure for BET measurements. Four grams of ZnO (Alfa Aesar 99.99%) were taken for experiments to increase detection limits. Two experiments were performed on the same sample. Initially, the sample was degassed at 450 °C for 10 h under active evacuation and backfilled at 25 °C with 2.7 kPa of water vapor, evacuated at room temperature for 6 h and then exposed to CO_2 at the same pressure. Concentrations of H_2O and CO_2 in the gas phase were qualitatively analyzed using the capillary input of the mass spectrometer. The procedure was repeated after another degas at 450 °C followed by exposure to CO_2.

3. RESULTS AND DISCUSSION

3.1. Powder Characterization. The powders prepared by laser evaporation were analyzed by XRD and the diffraction pattern was indexed as wurtzite-type ZnO without any metallic zinc or other impurities (Figure 1). A homogeneous particle

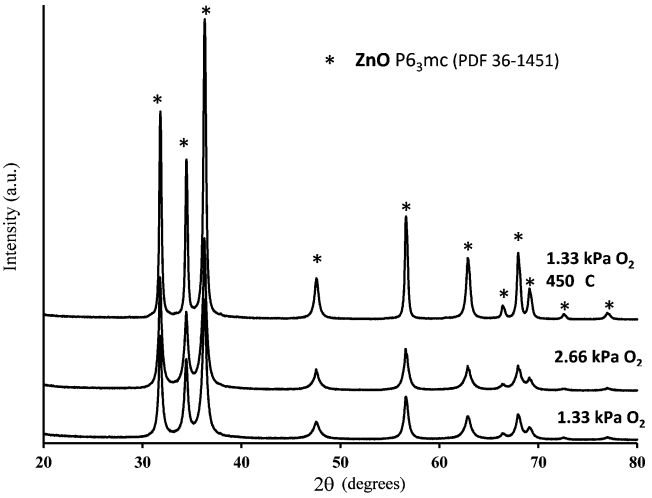

Figure 1. XRD patterns (Cu $K\alpha$ radiation) of ZnO nanoparticles prepared by laser evaporation at 1.33 or 2.66 kPa O_2 pressure and compared to 1.33 kPa O_2 powder heat treated at 450 °C under vacuum.

size distribution could be verified by TEM (see SI). The median particle size was 9 ± 4 and 12 ± 4 nm for oxygen pressure of 1.33 and 2.66 kPa, respectively. The crystallite sizes estimated from XRD line broadening were 12 ± 2 and 18 ± 2 nm, respectively (Table 1). For both powders, BET surface areas SA_{BET} were 26.9 ± 0.2 and 24.4 ± 0.2 m^2/g, respectively (Table 1). The powder prepared at 1.33 kPa oxygen pressure was chosen for the adsorption study due to the higher specific surface area and the high evaporation rate during synthesis (Figure 2 and Table 1). For the powder heat treated in vacuum for 1 h, the SA decreased continuously with temperature as a consequence of particle growth (Figure 3). These results are consistent with previous report[17] of ZnO nanopowders preparation by laser evaporation in comparable conditions. The interface area, $IA = 0.5\cdot(SA_{TEM} - SA_{BET})$, and the ratio of interface area to surface area equal to one (IA/SA = 1.0) reveal a highly agglomerated as-prepared powder. After heat treatment at 450 °C, the particles grew and the total surface area was 3.5 times smaller than the original area, and the final interface/surface ratio became 0.5 (CTIA/SSA = 0.5, Table 1). The presence of grain boundaries was also observed by TEM. Initial adsorption calorimetry experiments were performed on as-prepared powders loaded into adsorption tubes inside the glovebox and degassed by evacuation at room temperature. The low coverages and adsorption enthalpies obtained on as-prepared ZnO samples (Table 2) indicated that despite handling in the glovebox, the surfaces of as-prepared powders contained some adsorbed species. Thermogravimetry con-

dx.doi.org/10.1021/la500743u | Langmuir 2014, 30, 9091−9097

Table 1. Median Particle Size from TEM, Crystallite Size from XRD, BET Surface Area (SA_{BET}), Calculated Surface Area from Particle Size (SA_{TEM}) and Calculated Interface Area ($IA = 0.5 \cdot (SA_{TEM} - SA_{BET})$) for ZnO Prepared by Laser Evaporation

sample	median particle size TEM (nm)	crystallite size XRD (nm)	SA_{BET} ($m^2 \cdot g^{-1}$)	SA_{TEM} ($m^2 \cdot g^{-1}$)	interface area (IA) ($m^2 \cdot g^{-1}$)	IA SA
1.33 kPa O_2	9 ± 4	12 ±2	26.9 ± 0.2	82.3	28	1.0
2.66 kPa O_2	12 ± 4	18 ±2	24.4 ± 0.2	72.5	24	1.0
1.33 kPa O_2 450 °C/4 h	40 ± 10	48 ±6	11.5 ± 0.1	23.7	6	0.5

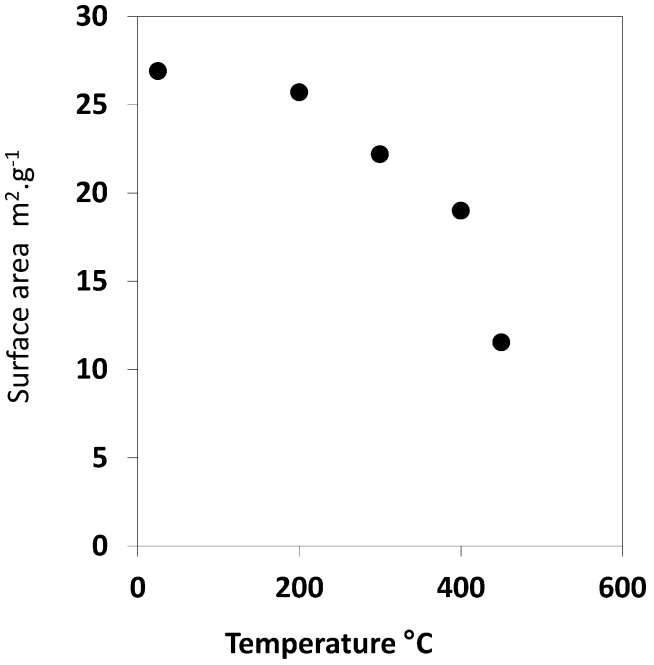

Figure 2. Specific surface area determined by N_2 adsorption for ZnO prepared at 1.33 kPa O_2 pressure heat treated for 4 h at different temperatures under vacuum.

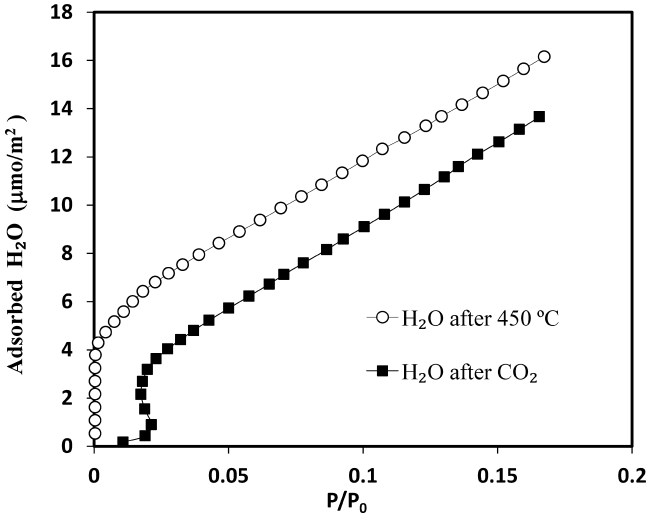

Figure 3. Adsorption isotherms of water vapor on ZnO nanopowders, heat treated for 4 h at 450 °C under vacuum, and after CO_2 adsorption and evacuation at 25 °C.

firmed this assumption and mass spectometry of evolved gas during TPD experiments indicated the presence of both H_2O and CO_2 on the as-prepared powders. Adsorption data obtained on as-prepared powders are not further discussed here but are presented in the SI.

Table 2. Molecular Coverage, Integral Heat of Adsorption, Differential Heat of Adsorption for the First Dose during Water and CO_2 Isotherm Adsorption at 25 °C on ZnO Powder Prepared by Laser Evaporation

isotherm 25 °C	coverage molecules/nm^2	integral heat of adsorption kJ/mol	differential heat of adsorption (first dose) kJ/mol
H_2O as prepared	2.3	−54.0 ± 1.4	−98.2
H_2O after 450 °C	5.6	−96.8 ± 2.5	−159.1
H_2O after CO_2	4.0	−73.5 ± 1.9[a]	−309.5[a]
CO_2 as prepared	1.1	−36.3 ± 1.0	−54.3
CO_2 after 450 °C	2.6	−96.6 ± 2.5	−119.7
CO_2 after H_2O	0.9	−47.4 ± 1.2	−115.1

[a]CO_2 desorption was detected

In previous experimental adsorption studies by Nagao et al.,[14−16] Zhang et al.,[10] Shvareva et al.,[11] and Gervasini et al.,[9] degas conditions for ZnO were 400−500 °C. The choice of the temperature was often based on thermogravimetry measurements of ZnO powders, which show minor weight loss above 450 °C,[10] attributed to ZnO loss by evaporation. The degas at higher temperature would decrease surface area substantially, reducing accuracy and resolution of differential adsorption enthalpy measurements. Thus, in our experiments ZnO powders for adsorption studies were degassed at 450 °C.

3.2. CO_2 and H_2O Adsorption after Degas at 450 °C.

H_2O and CO_2 adsorption isotherms at 25 °C are shown in Figures 3 and 4. The vertical segment of isotherms at low coverage indicates strong chemisorption where ZnO surfaces

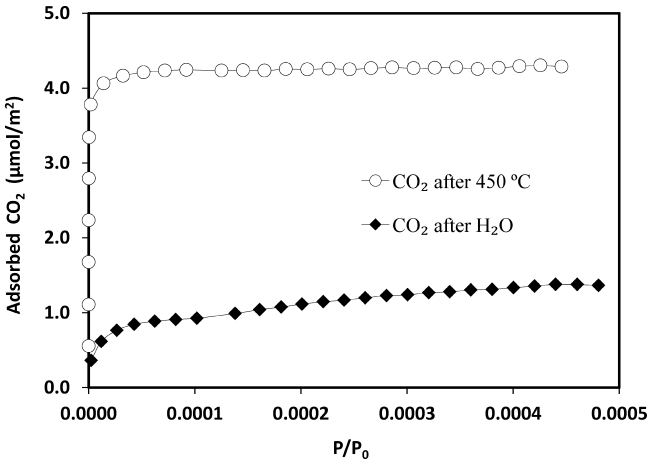

Figure 4. Adsorption isotherms of CO_2 on ZnO nanopowders heat treated for 4 h at 450 °C under vacuum, and after H_2O adsorption and evacuation at 25 °C.

dx.doi.org/10.1021/la500743u | Langmuir 2014, 30, 9091−9097

absorb all the gas to which they are exposed. In both cases, an increase in pressure is only observed when 4 μmol/m^2 were adsorbed. Adsorption of CO_2 effectively stops at this coverage and isotherm becomes flat. Water adsorption proceeds with corresponding pressure increase. Simultaneous measurements of adsorption enthalpies per dose are shown in Figure 5 with

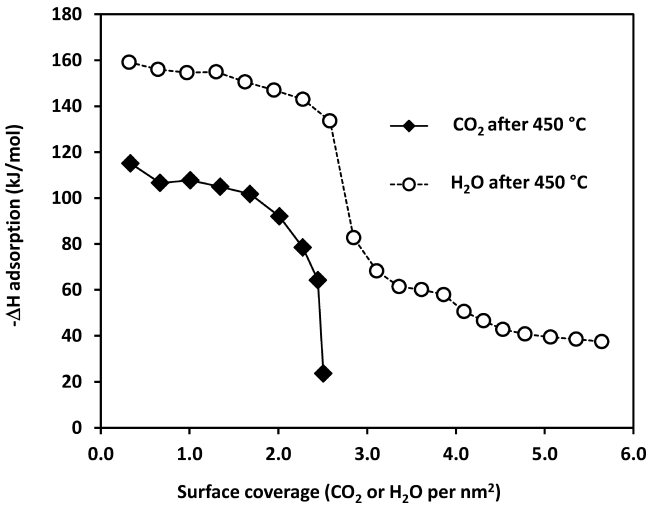

Figure 5. Differential enthalpies of adsorption of water and CO_2 versus ZnO surface coverage after 450 °C degas.

coverages recalculated to H_2O and CO_2 per nm^2. Differential enthalpy of adsorption for CO_2 changes from −120 to −100 kJ/mol and drops rapidly in magnitude when coverage reach 1.7 CO_2/nm^2, giving a value of −107.2 kJ/mol for the integral enthalpy of adsorption. This value is in excellent agreement with the value of −103.4 kJ/mol measured by Gervasini and Auroux[8,9] for the same coverage for samples prepared by a different method and using a custom-made gas dosing system. This agreement validates our experimental procedure and indicates that, after heat treatment at 450 °C, surfaces of ZnO powders from laser evaporation do not exhibit any unique properties and thus our results can be applied for clean polycrystalline ZnO surfaces obtained by different methods. In the case of noncondensing adsorbents such as CO_2, the value for integral adsorption enthalpy will depend on the coverage when adsoprtion is ceased. The determination of the coverage is affected both by dosing amounts and sensitivity of calorimetric heat evolution detection. Our value of integral enthalpy of adsorption of CO_2 listed in Table 2 is −96.6 ± 2.5 kJ/mol corresponds to a coverage of 2.6 CO_2/nm^2.

Differential enthalpy of water adsorption is more negative than for CO_2 at all coverages (Figure 5). Notably, a step in differential adsorption enthalpy is observed around 2.5−3 H_2O/nm^2 coverage when CO_2 adsorption ceases. Water adsorbs with an enthalpy of −160 to −140 kJ/mol until 2.5 H_2O/nm^2, while after a coverage of 3 H_2O/nm^2 is reached, the values become less exothermic than −60 kJ/mol. Our measurements give the integral enthalpy of chemisorption of water as −96.8 ± 2.5 kJ/mol for a coverage of 5.6 H_2O/nm^2. Since H_2O is a condensable adsorbent, the integral enthalpy of chemisorption is calculated as the total heat evolved divided by total adsorbed moles of H_2O up to the coverage where the enthalpy of adsorption per dose reaches the enthalpy of condensation (−44 kJ/mol).

To account for any water adsorption outside of the sample, a correction for water adsorption on empty tube is applied from a blank experiment. This correction does not affect the differential enthalpy of adsorption at low pressure for a strong chemisorption case, like ZnO, when the sample acts as an effective gas getter, but this correction becomes more important for the integral enthalpy of adsorption calculation and estimation of coverage for chemisorbed water. For comparison of water adsorption results, we note that uncertainties in surface area measurements do not affect integral chemisorption enthalpies calculated for water, but correction for adsorption on the tube does. The value for coverage is additionally affected by uncertainty in surface area measurement.

Water adsorption on ZnO was previously measured at the UC Davis Thermochemistry Laboratory using the same instrumentation but different samples. Zhang et al.[10] reported enthalpies of H_2O adsorption on ZnO nanoparticles and nanorods prepared by different methods. They found different profiles of differential enthalpies of adsorption vs coverage for these samples, but similar integral enthalpies of adsorption around −100 kJ/mol for a coverage of 5 H_2O/nm^2. For both samples, they reported differential enthalpies of the first two doses of −400 to −600 kJ/mol. They used the same degas temperature of 450 °C but doses ∼3 times smaller than in the present work. Their integral enthalpies of adsorption are slightly higher but in reasonable agreement with the present study and the apparently higher enthalpies of adsorption of first doses are likely to contribute to this discrepancy.

Measurement of adsorption enthalpies for the first doses at low pressure requires equilibration time often in excess of 1 h per dose, since heat transfer from the sample to the forked tube is mostly by heat conduction and not by both conduction and convection as at higher pressures. However, the leak rate at low pressures is the highest which can result in abnormally high apparent enthalpies of adsorption for first doses in the Zhang et al.[10] experiments. Since then, experimental procedure was modified to alleviate this effect by increasing the dose amounts at low pressure. A later set of measurements of H_2O adsorption on ZnO was reported by Shvareva et al.[11] These were performed on the same instrument and degas condition but for ∼5 nm ZnO nanoparticles prepared by atomic layer deposition on an amorphous silica substrate. Much larger doses were used; all chemisorption was accomplished in 4 doses, and the first dose provided a coverage of ∼1.7 H_2O/nm^2 with enthalpy of adsorption about −150 kJ/mol. Reported integral adsorption enthalpies were in the range from −80 to −95 kJ/mol for coverage of 7.4 H_2O/nm^2. This is in remarkable agreement with our present data, and indicates that the integral enthalpy of water adsorption on ZnO surfaces treated above 450 °C is not significantly affected by the ZnO preparation method. Higher coverages reported in the work of Shvareva et al.[11] may be due to larger dose amounts.

It is remarkable that, despite close agreement with Zhang et al.[10] and Shvarevaet al.[11] in integral enthalpies of adsorption of H_2O on ZnO, the distinct step in differential enthalpy of adsorption of H_2O at 3 H_2O/nm^2 was not observed in those previous studies. Such a step would not be expected to be seen in the work of Shvareva et al.[11] due to large dose amounts; however, it should not have be missed by Zhang et al.[10] since they used smaller doses then in our experiment. Thus, we conclude that this difference is real and may reflect more distinct crystal faces formed during condensation from the gas phase, consistent with TEM observations.

dx.doi.org/10.1021/la500743u | *Langmuir* 2014, 30, 9091−9097

Two surfaces with low index and low surface energy planes are generally accepted as dominant on nano-ZnO: $(11\bar{2}0)$ and $(10\bar{1}0)$[10,18−21] and Zn site densities are 6.8 and 5.9 Zn/nm^2, respectively. Taking CO_2 cross sectional area[22] at 25 °C as 19 nm^2 a maximum coverage of 3.4 and 3.0 CO_2/nm^2 could be calculated for $(11\bar{2}0)$ and $(10\bar{1}0)$, respectively. The coverage obtained from the adsorption and calorimetric experiments after heat treatment at 450 °C was 2.6 CO_2/nm^2 and is thus relatively similar to the calculated values (Table 2). Two different adsorption sites could be inferred in the differential enthalpy of adsorption of H_2O after degas at 450 °C: the first site from 0.0 to 3.0 H_2O/nm^2 coverage is more energetic, and a second less strongly bound site from 3.0 to 6.0 H_2O/nm^2 (Figure 6). The two different sites agree well with surface

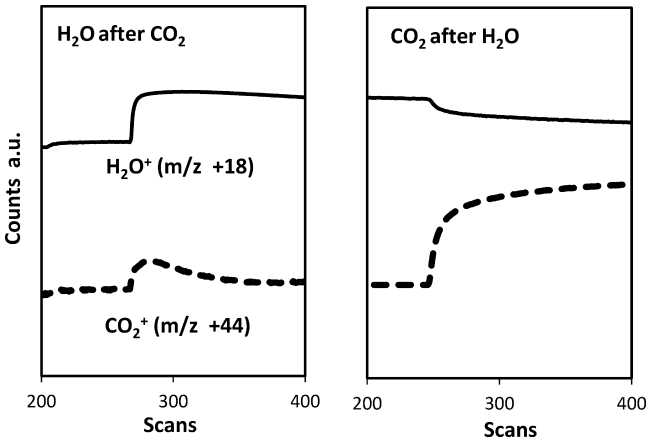

Figure 6. Mass spectrometry traces of H_2O and CO_2 during adsorption experiments. Left: Exposure to H_2O of the sample with adsorbed CO_2 on the surface. Right: Exposure to CO_2 of the sample with adsorbed water on the surface.

occupation for $(10\bar{1}0)$ which was calculated[23] to be 5.9 H_2O/nm^2. The binding energy of the half covered monolayer and the fully covered monolayer was calculated as 93.5 and 99.3 kJ/mol, respectively.[23] These results correlate well with our adsorption data: the half coverage shows a high energy of adsorption corresponding to water dissociation to form hydroxyl groups and full coverage corresponding to the less energetically adsorbed water molecules without any dissociation. Lacking new structural data, we do not speculate o the microscopic nature of these sites.

3.3. Effects of Preadsorbed Water and CO_2. Experiments were performed to reveal effects of H_2O on the surface on the adsorption of CO_2 and of the presence of CO_2 on the adsorption of H_2O. Mass spectrometry performed during adsorption on a bulk sample indicated partial desorption of CO_2 from ZnO when the sample was exposed to water vapor. No such effect was observed on exposure to CO_2 of the partially hydrated ZnO surface (Figure 6).

Figure 4 shows the CO_2 adsorption isotherm for ZnO exposed to water vapor and degassed at 25 °C. Total adsorbed amounts of CO_2 on the hydrated surface diminished by almost a factor of three compared to the surface without residual chemisorbed water. There is no well-defined vertical segment in the isotherm but adsorption proceeds to higher pressures (Figure 4). In contrast, the water adsorption isotherm does show a vertical segment with negative inflection. Mass spectrometry data indicate that adsorbed amounts of H_2O at low pressures are underestimated since preadsorbed CO_2 is partially released from the surface. This also results in overestimation of differential enthalpies of adsorption for the first doses of H_2O (Figure 7). Differential enthalpies of

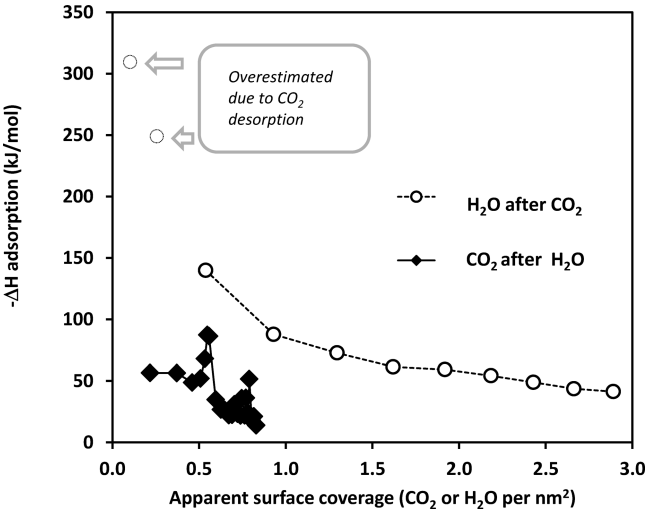

Figure 7. Differential enthalpies of adsorption of water and CO_2 versus ZnO surface coverage on surfaces exposed to water and CO_2 and degassed at 25 °C.

adsorption of CO_2 on the hydrated surface can only be detected up to a coverage less than 0.8 CO_2/nm^2 and show large scatter mostly due to low adsorbed amounts per dose, at the limit of detection of pressure transducers. Displacement of CO_2 by water on ZnO surfaces is consistent with the more negative initial enthalpy of water adsorption (−160 kJ/mol) compared with CO_2 (−140 kJ/mol).

3.4. Temperature-Programmed Desorption Mass Spectrometry (TPD-MS) Experiments. The TPD-MS results (see SI for details) show CO_2 and H_2O desorption from the as-prepared powder. H_2O desorption occurs at lower temperature (25−500 °C) than CO_2 (250−800 °C) and two peaks at different temperatures could be detected: a first large broad peak at 100−300 °C and a small peak at 500 °C. Three roughly equal CO_2 desorption peaks were seen: 380, 485, and 641 °C. Comparing results from TPD-MS and thermogravimetry, it is possible to verify that water is the most important component in the mass change during heating and that the first broad peak observed by TPD-MS is actually composed of two different mass losses. The first mass loss in the 25−150 °C range is associated with the physisorbed water. However, the second mass change at 150−800 °C is a combination of H_2O and CO_2 desorption, with the mass change at 500−800 °C mostly due to CO_2. It is important to note that some residual CO_2 could be found at higher temperature than adopted for degas conditions before gas adsorption. A similar high persistence of CO_2 adsorption has been found for MgO—ZrO_2 and MgO—TiO_2 solid solution nanopowders and glassy carbon surfaces by TPD-MS.[24]

CO_2 desorption persistence against the degas conditions before gas adsorption was tested by heat treating the powder at 450 °C for 5 h under vacuum and then carrying out TPD-MS from 450 to 800 °C. Figure 8 shows that only the last peak is observed and CO_2 still persists on ZnO nanopowder surfaces after degas treatment, suggesting a high energy of adsorption. An approximate calculation on the CO_2 desorption energy from

dx.doi.org/10.1021/la500743u | Langmuir 2014, 30, 9091−9097

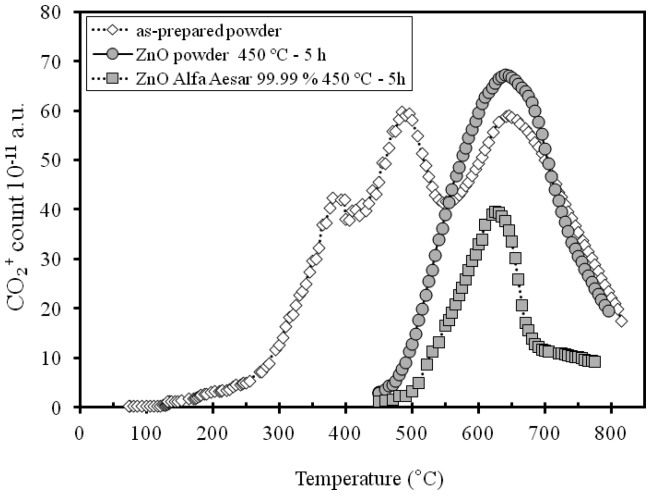

Figure 8. TPD-MS analysis of as-prepared ZnO powders, ZnO powder heat treated at 450 °C under high vacuum, and commercial ZnO powder heat treated at 450 °C under high vacuum.

the TPD-MS experiments was previously proposed for glassy carbon surfaces.[25] Taking into account similar conditions of desorption and using a heating rate of 10 °C min^{-1}, the energy of adsorption estimated for the last peak is about −200 kJ/mol, which is about twice the energy found for the low temperature CO_2 adsorption (Table 2). The residual SSA for a ZnO nanopowder heated to 645 °C at 10 °C/min and without soak time is 11.3 $m^2 \cdot g^{-1}$ which is similar to that for the powder heated at 450 °C for 5 h, so coarsening does not appear to be associated with this heat treatment and CO_2 evolution. TPD-MS analysis of ZnO nanopowder prepared by laser evaporation can be compared to that of commercial bulk ZnO powder (Alfa Aesar 99.99%) pretreated at 450 °C for 5 h (Figure 8). The results are similar.

TPD experiments have shown that at 450 °C under vacuum, it is possible to eliminate most of the moisture from the ZnO surface, but this is not true for CO_2. A highly persistent species, perhaps a stable carbonate ion, is formed on the ZnO surface and can be completely desorbed only at temperatures higher than 800 °C and under vacuum. The same persistent molecules were found on high purity commercial powder, showing that such adsorption is not limited to ZnO nanopowders prepared by laser evaporation (Figure 8). Indeed, adsorbed CO_2 and SO_2 have been detected on many oxide surfaces and desorption temperatures can be as high as 1000 °C.[24−26]

4. SUMMARY

Energetics of CO_2 and H_2O adsorption was studied on the same samples of polycrystalline ZnO powders. Synthesis by laser evaporation in oxygen ensured the absence of organic and inorganic contaminants other than low levels of H_2O and CO_2 when samples were maintained in a nitrogen filled glovebox. Samples were heat treated at 450 °C in vacuum. Integral enthalpy of H_2O adsorption was measured as −96.8 ± 2.5 kJ/mol and enthalpy of water condensation was reached at 5.6 H_2O/nm^2. The differential enthalpy of H_2O adsorption is in the range −160 to −140 kJ/mol up to a coverage of 2.5 H_2O/nm^2. Adsorption of CO_2 on a sample degassed at 450 °C gives differential enthalpy of adsorption −120 to −100 kJ/mol which drops to zero abruptly when a coverage of 2.6 CO_2/nm^2 is reached, giving an integral adsorption enthalpy of −96.6 ± 2.5 kJ/mol. Adsorption of CO_2 on a partially hydrated ZnO surface results in lower coverage and integral enthalpy of adsorption of −47.4 ±1.2 kJ/mol at 0.9 CO_2/nm^2. Adsorption of H_2O on a surface with preadsorbed CO_2 causes partial displacement of CO_2 from ZnO surfaces as evident from gas analysis. However, temperature-programmed desorption experiments performed both on bulk ZnO and the as-prepared nanophase powders indicated that some CO_2 is retained above 450 °C and desorbed up to 800 °C, with estimated adsorption energies near −200 kJ/mol. Our data indicate that zinc oxide surfaces act as a strong getter both for water and CO_2 with H_2O coverages and energies typical for dissociative adsorption on oxide surfaces. When exposed to atmospheric, or even low level concentrations of water and carbon dioxide, such as in a nitrogen filled glovebox, both H_2O and CO_2 will adsorb on the ZnO surface. The most strongly bound CO_2 remains after prolonged degas at 450 °C, when all water is desorbed. However, some sites active to CO_2 adsorption will exchange readily for water. Apart from the observed competition between H_2O and CO_2 for a small fraction of surface sites, our data do not indicate that H_2O or CO_2 present on the surface cause any anomalous change in coverage of the other gas.

■ ASSOCIATED CONTENT

Ⓢ Supporting Information

(Figure S1) The chamber used for synthesis of ZnO by laser evaporation. (Figure S2) Bright field TEM micrographs of ZnO samples prepared by condensation from gas phase. (Figure S3) Particle size distribution measured by TEM of ZnO nanoparticles prepared by laser evaporation. (Figure S4) Experimental arrangement for gas adsorption calorimetry measurements. (Figure S5) Adsorption isotherms of water vapor at 25 °C on as-prepared ZnO nanopowders. (Figure S6) Differential enthalpy of adsorption per mole of H_2O vs surface coverage for as-prepared ZnO nanopowders. (Figure S7) Adsorption isotherms of carbon dioxide on as-prepared ZnO nanopowders. (Figure S8) Differential heat flow versus CO_2 coverage. (Figure S9) Experimental arrangement for temperature programmed desorption (TPD) measurements. (Figure S10) Temperature-programmed desorption (TPD) method combined with mass spectrometric (MS) analysis of as-prepared ZnO powder compared with empty tube. (Figure S11) Thermogravimetric (TG)analysis of as-prepared ZnO powder compared to TPD-MS results. This material is available free of charge via the Internet at http://pubs.acs.org.

■ AUTHOR INFORMATION

Corresponding Author

*E-mail: anavrotsky@ucdavis.edu.

Notes

The authors declare no competing financial interest.

■ ACKNOWLEDGMENTS

D.G. thanks FAPESP (Process Number 05/53241-9 and 11/02080-6) for financial support. This work was supported at UC Davis by the U.S. Department of Energy—Program: Basic Energy Science (DOE-BES)—Grant Energetics of Nanomaterials (DE-FG02-05ER15667).

■ REFERENCES

(1) Inoue, T.; Fujishima, A.; Konishi, S.; Honda, K. Photoelectrocatalytic Reduction of Carbon Dioxide in Aqueous Suspensions of Semiconductor Powders. *Nature (London)* **1979**, *277*, 637−638.

(2) Watanabe, M. Photosynthesis of Methanol and Methane from CO_2 and H_2O Molecules on a ZNO Surface. *Surf. Sci.* **1992**, *279*, L236−L242.
(3) Abanades, S. P.; Chambon, M. CO_2 Dissociation and Upgrading from Two-Step Solar Thermochemical Processes Based on ZnO/Zn and SnO_2/SnO Redox Pairs. *Energy Fuels* **2010**, *24*, 6667−6674.
(4) Doh, W. H.; Roy, P. C.; Kim, C. M. Interaction of Hydrogen with ZnO: Surface Adsorption versus Bulk Diffusion†. *Langmuir* **2010**, *26*, 16278−16281.
(5) Gálvez, M. E.; Loutzenhiser, P. G.; Hischier, I.; Steinfeld, A. CO_2 Splitting via Two-Step Solar Thermochemical Cycles with Zn/ZnO and FeO/Fe_3O_4 Redox Reactions: Thermodynamic Analysis. *Energy Fuels* **2008**, *22*, 3544−3550.
(6) Smestad, G. P.; Steinfeld, A. Review: Photochemical and Thermochemical Production of Solar Fuels from H_2O and CO_2 Using Metal Oxide Catalysts. *Ind. Eng. Chem. Res.* **2012**, *51*, 11828−11840.
(7) Stamatiou, A.; Loutzenhiser, P. G.; Steinfeld, A. Solar Syngas Production via H_2O/CO_2-Splitting Thermochemical Cycles with Zn/ZnO and FeO/Fe_3O_4 Redox Reactions†. *Chem. Mater.* **2009**, *22*, 851−859.
(8) Auroux, A.; Gervasini, A. Microcalorimetric Study of the Acidity and Basicity of Metal-Oxide Surfaces. *J. Phys. Chem.* **1990**, *94*, 6371−6379.
(9) Gervasini, A.; Auroux, A. Acidity and Basicity of Metal-Oxide Surfaces. 2. Determination by Catalytic Decomposition of Isopropanol. *J. Catal.* **1991**, *131*, 190−198.
(10) Zhang, P.; Xu, F.; Navrotsky, A.; Lee, J. S.; Kim, S. T.; Liu, J. Surface Enthalpies of Nanophase ZnO with Different Morphologies. *Chem. Mater.* **2007**, *19*, 5687−5693.
(11) Shvareva, T. Y.; Ushakov, S. V.; Navrotsky, A.; Libera, J. A.; Elam, J. W. Thermochemistry of Nanoparticles on a Substrate: Zinc Oxide on Amorphous Silica. *J. Mater. Res.* **2008**, *23*, 1907−1915.
(12) Webb, P. A.; Orr, C. *Analytical Methods in Fine Particle Technology*; Micromeretics Instrumnt Corp.: Norcross, 1997.
(13) Ushakov, S. V.; Navrotsky, A. Direct Measurements of Water Adsorption Enthalpy on Hafnia and Zirconia. *Appl. Phys. Lett.* **2005**, *87*, 164103/1−164103/3.
(14) Nagao, M. On Physisorption of Water on Zinc Oxide Surface. *J. Phys. Chem.* **1971**, *75*, 3822−3828.
(15) Nagao, M.; Kumashiro, R.; Matsuda, T.; Kuroda, Y. Calorimetric Study of Water 2-Dimensionally Condensed on the Homogeneous Surface of a Solid. *Thermochim. Acta* **1995**, *253*, 221−233.
(16) Nagao, M.; Yunoki, K.; Muraishi, H.; Morimoto, T. Differential Heat of Chemisorption. 1. Chemisorption of Water on Zinc-Oxide and Titanium-Dioxide. *J. Phys. Chem.* **1978**, *82*, 1032−1035.
(17) Eilers, H.; Tissue, B. M. Synthesis of Nanophase ZnO, Eu_2O_3, and ZrO_2 by Gas-Phase Condensation with cw-CO_2 Laser Heating. *Mater. Lett.* **1995**, *24*, 261−265.
(18) Marana, N. L.; Longo, V. M.; Longo, E.; Martins, J. B. L.; Sambrano, J. R. Electronic and Structural Properties of the (1010) and (1120) ZnO Surfaces. *J. Phys. Chem. A* **2008**, *112*, 8958−8963.
(19) Na, S.-H.; Park, C.-H. First-Principles Study of the Surface of Wurtzite ZnO and ZnS—Implications for Nanostructure Formation. *J. Korean Phys. Soc.* **2009**, *54*, 867−872.
(20) Diebold, U.; Koplitz, L. V.; Dulub, O. Atomic-Scale Properties of Low-Index ZnO Surfaces. *Appl. Surf. Sci.* **2004**, *237*, 336−342.
(21) Morimoto, T.; Nagao, M. Adsorption Anomaly in System Zinc Oxide-Water. *J. Phys. Chem.* **1974**, *78*, 1116−1120.
(22) McClella, Al; Harnsber, Hf Cross-Sectional Areas of Molecules Adsorbed on Solid Surfaces. *J. Colloid Interface Sci.* **1967**, *23*, 577−599.
(23) Meyer, B.; Marx, D.; Dulub, O.; Diebold, U.; Kunat, M.; Langenberg, D.; Woll, C. Partial Dissociation of Water Leads to Stable Superstructures on the Surface of Zinc Oxide. *Angew. Chem., Int. Ed.* **2004**, *43*, 6642−6645.
(24) Aramendia, M. A.; Borau, V.; Jimenez, C.; Marinas, A.; Marinas, J. M.; Ruiz, J. R.; Urbano, F. J. Magnesium-Containing Mixed Oxides as Basic Catalysts: Base Characterization by Carbon Dioxide TPD-MS and Test Reactions. *J. Mol. Catal. A-Chem.* **2004**, *218*, 81−90.
(25) Peric-Grujic, A. A.; Neskovic, O. M.; Veljkovic, M. V.; Lausevic, M. D.; Lausevic, Z. V. A TPD-MS study of glassy carbon surfaces oxidized by CO_2 and O^-_2. *J. Serbian Chem. Soc.* **2002**, *67*, 761−768.
(26) Li, F.; Yan, B.; Zhang, J.; Jiang, A. X.; Shao, C. H.; Kong, X. J.; Wang, X. Study on Desulfurization Efficiency and Products of Ce-Doped Nanosized ZnO Desulfurizer at Ambient Temperature. *J. Rare Earths* **2007**, *25*, 306−310.